J Solid State Electrochem (2005) 9: 30–42
DOI 10.1007/s10008-004-0531-z

ORIGINAL PAPER

W. T. Tan · E. B. Lim · J. K. Goh

Voltammetric studies of microcrystalline C_{60} adhered to a carbon electrode surface and placed in contact with aqueous electrolyte containing potassium ions

Published online: 29 May 2004

Abstract The reduction of microcrystalline C_{60}fullerene, adhered at a carbon electrode and immersed in aqueous electrolyte, has been studied under various voltammetric conditions. This work reports mainly the voltammetric studies carried out principally in electrolyte containing potassium ions. Comparison of adherence techniques, such as solvent casting and mechanical transfer methods, are made to assess if the type of adhered techniques has any significant influence on the observed electrochemistry. The solvent casting method is found to produce three peaks in the potential for $C_{60}^{0/n-}$ redox couple as compared to a single and large peak produced when a mechanical transfer technique is employed. When the reduction potential of microcrystalline C_{60} in the presence of K^+ is compared with other cations, such as Li, Na, Rb and Cs, it is observed that the shift of reduction potential follows the change in the hydration energy in the order Cs > Rb > K > Na > Li. In a mixed electrolyte study of CsCl/KCl, the reduction potential and peak shape of $C_{60}^{0/n-}$ redox couple during cyclic voltammetry is observed to change with concentration of the cations and the observed electrochemistry can be attributed to a cation-exchange mechanism. The reduction of C_{60} is irreversible in aqueous electrolyte containing alkaline cations as the re-oxidation process does not produce any observed electro-activity. Evidence of the formation of a passive coating of K_nC_{60} fulleride, which does not appear to undergo dissolution is obtained under cyclic voltametric conditions. This coating remains electrochemically active in the presence of tetrabutylammonium ions in acetonitrile. Scan rate, chronocoulometric, and scanning electron microscopic studies provide evidence of the presence of a surface process involving solid–solid transformation.

W. T. Tan (✉) · E. B. Lim · J. K. Goh
Department of Chemistry, Universiti Putra Malaysia,
43400 UPM Serdang, Selangor D.E., Malaysia
E-mail: wttan@fsas.upm.edu.my
Fax: 603-89432508

Keywords C_{60} · Aqueous solution · Solvent casting · Mechanical transfer · Voltammetry

Introduction

The electrochemistry of C_{60} fullerenes in both the solution phase [1, 2, 3, 4, 5,6] and solid phase [7, 8, 9, 10, 11, 12, 13, 14, 15, 16, 17, 18, 19, 20, 21,22] voltammetry has been widely studied. The former include the determination of the electrochemical properties and the sixth reversible consecutive one-electron reduction steps in some non-aqueous solutions. Earlier voltammetric studies of a solid "film," obtained by adhering an array of microcrystalline C_{60} on the solid state electrode surface, describe how the reversibility of C_{60}redox reaction of the film is dependent on the size of cation in appropriate electrolytes (usually non-aqueous solvent) and to what extent the film is reduced. The study on the incorporation process of cations such as NBu_4^+ into the C_{60} microcrystal lattices under cyclic voltammetric time scale has detected evidence of nucleation and growth processes [14].

Although solid phase voltammetry of C_{60} in non-aqueous media is widely reported, it is less reported in aqueous media. Szucs et.al. have discussed some electrochemical properties of the fullerene films in aqueous media, including their reactivity, stability and effect of doping (including mixed doping), and their conductive behaviors as possible electrode materials [15, 16, 17, 18,19]. The influence of mixed solvents of aqueous/non-aqueous nature on the redox process of C_{60}(CTV)–tetrabutylammonium salt and C_{60} films have been discussed by Bond et al. [22] and Szucs et al. [23], respectively. A related chemical system where a solid state reaction that is irreversible has become reversible on the addition of a redox mediator has also been observed by Oyama [24].

Among the work mentioned above on C_{60}, those reported by Szucs et al. on C_{60} in aqueous media [15, 16, 17, 18,19] are closely related to this paper. However, they

appear to use only the solvent/solution casting (SC) technique for depositing microcrystals of C_{60} on a solid electrode surface. The mechanical transfer/abrasive technique has been widely used and was detected to produce some differences and similarities in the redox waveforms of C_{60} in non-aqueous solvent when compared to those obtained via solvent casting under different conditions [20]. In this work, we attempt to compare the electrochemical behaviors of C_{60} film in aqueous media using the two techniques. We also include the work done on chronoamperometry and chronocoulometry, morphological aspects of C_{60} in the presence of a dopant, and various other effects not previously reported.

Experimental

Chemicals and materials

C_{60} (Fluka, 98%, HPLC), alkali metal salts of perchlorate and chloride were used as received. All chemicals used were of analytical reagent grade and used without further purification.

Methods

The surface of the working electrode was renewed and cleaned during every experiment by using a polishing kit, followed by ultrasonic cleaning for about 2–3 min. It was then flashed with distilled water and acetone, and dried at ca. 40 °C.

Two methods were used to transfer solid C_{60} onto the working electrode surface. The first one was a mechanical attachment technique (MA). This method includes direct use of solid C_{60} in powder form, as mentioned in detail in [20]. The second method is known as the solvent casting (SC) method. It was done by evaporating a certain quantity (μL) of C_{60} solution onto the fresh working electrode surface. The solution of C_{60} was prepared by dissolving C_{60} in CH_2Cl_2 to form a brownish solution of 150 μM. A certain volume of this solution (20 μL unless stated otherwise) was then deposited onto the working electrode surface using a micro-syringe until the whole drop was consumed. An array of microcrystals of fullerene was formed and eventually cast on the electrode surface by successive fast drying of the C_{60} solution under 40°C hot air. The working electrode surface with a well-coated layer of C_{60} microcrystals was then tested with various voltammetric techniques.

Electrochemical apparatus

The voltammetric experiments were performed with the electrochemical workstation (Model BAS 50 W, Bioanalytical Systems, West Lafayette, Indiana, USA), which was controlled solely by external computer. A conventional three-electrode configuration (BAS model) was employed with platinum wire as the counter electrode and silver–silver chloride (Ag/AgCl, 3 M NaCl) as the reference electrode. The working electrode used was a 3 mm diameter glassy carbon (GC) disk.

Scanning electron microscopy

A piece of basal plane pyrrolitic graphite (BPPG) electrode with diameter 5 mm, 2–3 mm thickness was cut from its rod and was polished with 320CW silicon carbide abrasive paper, followed by a further polishing with alpha-alumina (> 99.5% Al_2O_3) powder. Methods similar to those mentioned earlier for cleansing and deposition of microcrystals of C_{60} were then applied to the case where a BPPG electrode was used. To study the surface morphology of the compound after electrolysis, the BPPG electrode (with an array of C_{60} microcrystals attached to the surface) was then joined to a platinum wire as a conductor. The reduction potential was held at –1.800 V for 1 min in an appropriate electrolyte using the bulk electrolysis mode of the electrochemical workstation (Model BAS 100 W). The scanning electron microscope model JEOL JSM-6400 (Philips) was used to study the surface morphology of C_{60} before and after electrolysis.

In situ electrochemical optical microscopic studies were performed using a modulated Inverted optical microscope and a electrochemical workstation (BAS 50 W).

Results and discussion

Cyclic voltammograms of C_{60}adhered to electrode surface via mechanical attachment and solvent casting

Figure 1 shows the cyclic voltammograms of C_{60} attached onto a 3 mm GCelectrode via mechanical attachment and solvent casting methods. In the former case, as shown in Fig. 1a, its *i* - *E*curve is characterized by one large and sharp peak appearing at –1470 mV with a shoulder appearing as a pre-peak at –1100 mV. In the latter case, as shown in Fig. 1b, it is characterized by the presence of three peaks, which are not completely resolved as the lower regions of the reduction peaks overlap each other. The first small peak (i), the second large peak (ii) and the third peak (iii) appear at –1410 mV, –1520 mV, and -1737 mV, respectively (Fig. 1b). In both the adhered techniques, a complete absence of electro-activity is observed on re-oxidation, indicating that the reduction process is irreversible (to be elaborated latter). It is also observed that a rapid decrease in the electro-activity in subsequent potential cycling is similar to that reported earlier [15, 16]. The present study of $C_{60}^{0/n-}$ in aqueous media is therefore different from the case of $C_{60}^{0/n-}$ in non-aqueous media of NBu_4PF_6 /acetonitrile where continuous electroactivity can be observed during potential cycling. For

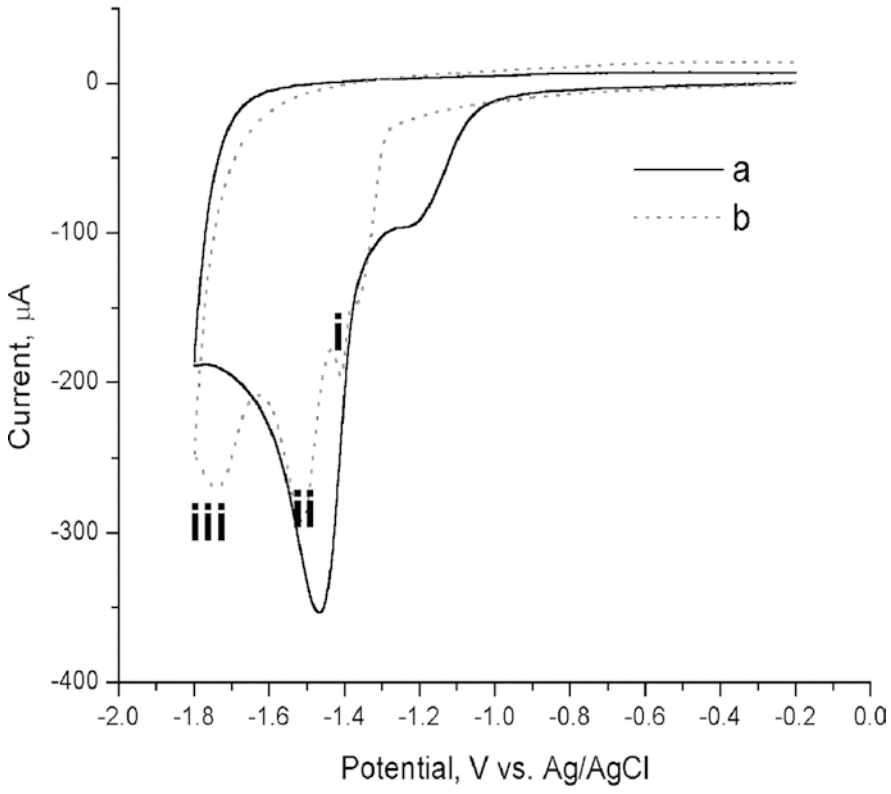

Fig. 1 Cyclic voltammograms of solid C_{60} attached onto 3 mm diameter GC electrode surface by (*a*) mechanical attachment of C_{60} microcrystals, (*b*) solvent casting of 20 μL C_{60} /CH_2Cl_2 and immersed in 0.1 M KCl using a scan rate of 100 mV/s

the latter case, both the MT and SC techniques of solid deposition produce dissimilar voltammetric behaviors during initial cycling. However, after the third cycle, both techniques produce similar voltammetric behaviors that are associated with steady-state conditions [14, 20]. The surprisingly reproducible nature of the cyclic voltammograms of the C_{60} aqueous system during the initial cycle and their usefulness has therefore prompted us to report the findings, despite the fact that there is a lack of confirmation that the cyclic voltammogram obtained during first cycle has attained a steady state condition (Fig. 1).

In case (a) for mechanical attachment, the current is larger, and may not be a simple one-electron reduction process and, since the total amount of microcrystal of C_{60} attached is unknown, it is not possible to calculate the charge transferred per molecule. The presence of three separate peaks as shown in case (b) for solvent casting, demonstrates the occurrence of more than one reduction process within the working range of –200 to –1800 mV. Based on calculation, 20 μL of 150 μM C_{60}/CH_2Cl_2solvent casted on a 3 mm diameter GC disk electrode has an equivalent of 4.3×10^{-8} mole C_{60} per cm^2 (mole per unit area of electrode surface), and the number of electrons transferred per molecule is close to 3. Although this value indicates a three-electron reduction of $C_{60,}$ via either one step or several consecutive one-electron steps, producing K_3C_{60} or K_nC_{60} (n =1–6), respectively, it has been pointed out by Szucs et al. (1997) that the electrochemical reaction may be rather complex. A mixture of K_nC_{60} (n =1–6) is thought to be formed, rather than a single or pure fulleride [18]. Two stable forms of C_{60} can be present in the final product: the conducting C_{60}^{3-} as K_3C_{60} and the semi-conducting C_{60}^{6-} as K_6C_{60}. The formation of K_3C_{60} fullerides is structurally more favorable as it requires only a slight rearrangement and expansion of the C_{60} crystals structure [8]. Disproportionation of KC_{60} into mainly the K_3C_{60} specie has been noted previously [8].

Due to the relatively large current, compare to a simple one-electron transfer process, it is believed that every reduction peak for C_{60} in case (b) and the single but large peak in case (a) are correlated to a multi-electron transfer process involving several consecutive one-electron reduction steps [14].

In case (b) where the SC deposition technique is employed, the distance between peaks (i) and (ii), and peaks (ii) and (iii) are ~100 mV and ~200 mV, respectively, which are sufficiently large at a scan rate of 100 mV/s. Consequently these three peaks are distinguishable although they overlap and merge near the half-wave peak. It indicates that the current for every single peak may include the current contributed by the nearby reaction.

However, in case (b) where MT is employed, it is probable that the peak separation (if any) is so small in a reduction process that the individual peaks cannot be distinguished from one another. The peaks coalesce to form one broad peak, hence the resultant i - E curve is the sum of individual i -E curves for each reduction step. In this case, the surface area or the total charge transferred under the CV plot is contributed by a mixture of those K_nC_{60} formed (n =1–6), and the peak potential observed is an average of the whole process.

The difference between the reduction waveform and qualitative pattern of C_{60} of different surface morphology and physical structure (MA and SC) can be explained by the difference in the connection between the particles, which determines the overall conductivity of the films [15].

Neither case (a) nor case (b) shows the oxidative current for the related $C_{60}^{0/-n}$ couple. In previous work, the absence of a re-oxidation wave has been attributed to either the dissolution of alkali-metal fulleride in acetonitrile [10] or to the formation of irreversible or non-electroactive compounds [11], however, the media used was non-aqueous. Szücs et al. have pointed out their view on the formation of irreversible compounds in aqueous media.

It is known that the secondary reduction processes may form a real protective layer on the outer surface of the film, preventing its complete degradation and thus allowing its further use in electrocatalysis [21]. This is true since electro-activity of $C_{60}^{0/-/2-}$ has almost disappeared, because of the presence of significantly larger background of the second and third cycles that is slightly higher than the background current during the initial scan. The larger background current is probably caused by the charging current of the electrode and the presence of an electro-inactive film of C_{60} salts.

Furthermore, investigation of the reduction of solid C_{60}, in aqueous solution containing 0.1 M K^+ under in situ electrochemical optical microscope (20× magnification), shows that there is no dissolution of the compound as the C_{60} compounds are still attached on the electrode surface after continuous potential cycling. Thus, it is clear that the loss of faradaic current of K_nC_{60} on the reversal sweep is not due to the dissolution, but rather the formation, of a passive coating of irreversible or non-electro-active salts as mentioned in earlier work [15]. Further evidence is given below on the continuing presence of the unoxidized K_n C_{60} species forming an electro-inactive species/passive coating on the electrode surface during re-oxidation of C_{60}^{n-}.

Effect of electrolyte on re-oxidation of the reduced C_{60}^{n-} film

The investigation of electrochemical behavior of re-oxidized fulleride species in different electrolyte is carried out as follows: An array of microcrystalline C_{60} attached mechanically on the 1 mm gold electrode is first reduced in 0.1 M KCl/H_2O, followed by the second reduction in a fresh, non-aqueous system of 0.1 M NBu_4PF_6/ACN. Figure 2a shows the reduction of microcrystalline C_{60} in 0.1 M KCl/H_2O; after the first cathodic wave, no oxidative current is observed on the reverse scan, and the electroactivity of $C_{60}^{0/n-}$ is totally lost on subsequent cycling. The irreversible reaction of $C_{60}^{0/n-}$ in K^+ electrolyte can be described by Eq. 1 (Fig. 2a). The same electrode with the reduced and re-oxidized C_{60} sample is then taken out, washed with a small portion of distilled water, followed by acetonitrile, and the reduction process is repeated in acetonitrile (0.1 M NBu_4PF_6). Interestingly, the familiar redox cyclic voltammograms of $(NBu_4)_nC_{60}$species ($n = 1, 2$) were obtained [7, 10, 11, 14,20]. The redox currents continue to increase on initial potential cycling (Fig. 2b) indicating the presence of C_{60} species in the re-oxidized film (to be explained further). Consequently, the "dissolution of K_nC_{60}" cannot be the reason for the loss of current in aqueous medium. This experiment confirms the presence of an array of reduced microcrystalline K_nC_{60} species, which are still held on the electrode surface after the reduction step, forming electro-inactive species that prevent further electrochemical activity. The stepwise reductions of K_nC_{60} in NBu_4^+/ACN appears reversible since on re-oxidation, well-defined oxidation peaks are observed (Eqs. 2 and 3) and appear similar to those observed previously [7, 10, 11, 14, 20]. After the completion of potential cycling experiments in NBu^{4+}/ACN, the electrode coated with C_{60} (B) (solid) is transferred to 0.1 M KCl solution for further cyclic voltammogram experiments. Similar irreversible reaction of $K_nC_{60,}$ as described by Eq. 4 is evident (Fig. 2c).

As noted above, continued increase in the redox currents was observed, as described by Eqs. 2 and 3, during the potential cycling experiment of K_nC_{60}-coated electrode in NBu_4^+/ACN. It can be attributed to an increasing conversion of K_n C_{60} to $(NBu_4^+)_nC_{60}$, probably via an ion exchange reaction that takes place between the mobile NBu_4^+ and the K^+ of the K_x C_{60} microcrystals formed previously (Eqs. 5 and 6 The ion exchange involving the conversion of K_nC_{60} to $(NBu_4^+)_2C_{60}$ appears to be incomplete in one potential cycle. Further potential cycling allows the ion exchange to be completed, as is reflected by a continuous increase in the redox peak current of $(NBu_4^+)_nC_{60}$species until a maximum peak current is reached after ten potential cyclings. A slightly slower kinetic of the ion exchange reaction reflects the presence of a rate-determining step involving the penetration of mobile NBu_4^+ into the lattice layers of K_n C_{60} microcrystals followed by a subsequent ion-exchange process between the mobile NBu_4^+ and the rigid, immobile K_nC_{60} layers.

Based on the models proposed by Jehoulet et al. [8] and Bond et al. [22] for the reactivity of C_{60}–tetrabutylammonium salt in non-aqueous solvent and for acetonitrile and C_{60} (CTV)–tetrabutylammonium salt in mixed solvent, the following scheme is proposed, which summarizes the redox reaction steps described above.

Electrochemical reduction of C_{60} microparticles in aqueous, non-aqueous, and aqueous solutions sequentially:

a. In 0.1 M KCl/H_20

   1. $C_{60(A)}$ (solid) + $nK^+ \rightarrow K_n$ C_{60}

b. In 0.1 M NBu_4PF_6/ACN

   2. x $[(NBu_4)_2C_{60}]$ (solid) $\rightleftharpoons$ x (NBu_4C_{60}) (solid) + x NBu_4^+ (solution) + x e^-

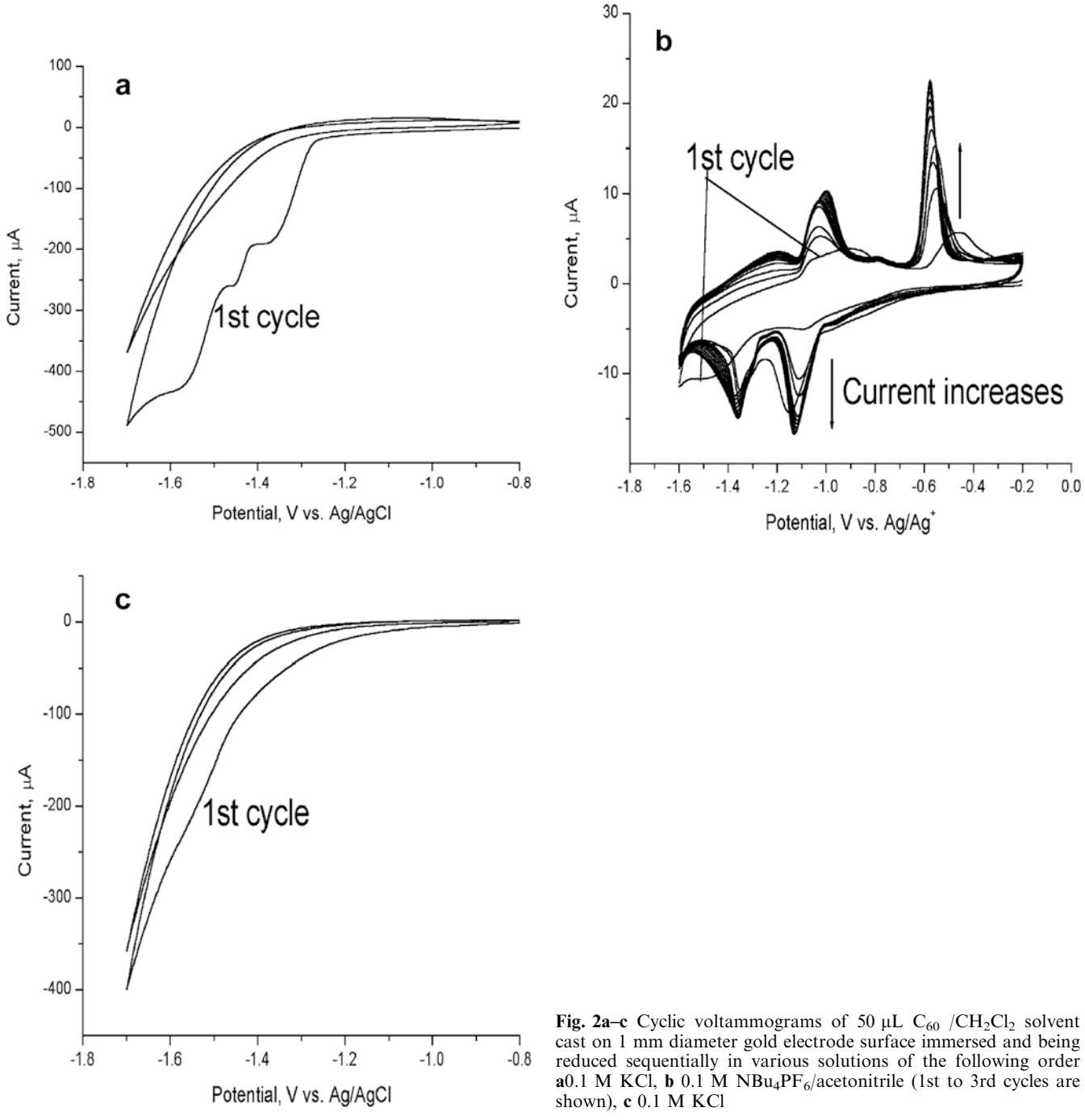

Fig. 2a–c Cyclic voltammograms of 50 μL C_{60} /CH_2Cl_2 solvent cast on 1 mm diameter gold electrode surface immersed and being reduced sequentially in various solutions of the following order **a**0.1 M KCl, **b** 0.1 M NBu_4PF_6/acetonitrile (1st to 3rd cycles are shown), **c** 0.1 M KCl

3. $x(NBu_4C_{60})$ (solid) $\rightleftharpoons x\ C_{60(B)}$ (solid) $+ x\ NBu_4^+$ (solution) $+ xe^-$

c. In 0.1 M KCl/H_2O again

4. $C_{60(C)}$ (solid) + $nK^+ \rightarrow K_nC_{60}$

Note that material A is probably associated with solvated structure of water, material B with solvated structure of acetonitrile, and material C with solvated structure of mixed solvent of water/acetonitrile.

d. Ion exchange reaction

5. $K_n\ C_{60}$ (solid) + x NBu_4^+ (solution) $\rightleftharpoons x[(NBu_4)C_{60}]$(solid) + (1- x) K_nC_{60} (solid) + $x\ K^+$ (solution)
6. $K_n\ C_{60}$ (solid) + $2xNBu_4^+$(solution) $\rightleftharpoons x[(NBu_4)_2 C_{60}]$(solid) + (1- x)K_nC_{60} (solid) + $x\ K^+$ (solution) ($x < 1$)

where x is the ratio of species formed, and this value increases with potential cycling. After several runs, if all

of the [K_n C_{60}] is converted to $(NBu_4)_2C_{60}$ and/or $(NBu_4)C_{60}$ at the end of the reduction process, then the value of *x*will be 1. As the process repeats, the amount of species $[C_{60}]_B$ increases and there will be less K_nC_{60} on the electrode surface. $[C_{60}]_B$ is to be differentiated from $[C_{60}]_A$ as they are different from one another in its film structure [8] and in our case, most likely in its solvated structure (as explained above). Furthermore, some of the compound may suffer some losses during the transfer and repetitive reduction process.

Consequently, cyclic voltammograms obtained for the same electrode coated with $[C_{60}]_B$ in 0.1 M KCl/H_2O again (Fig. 2c) shows only a much smaller reduction current, as compared with the earlier voltammogram (Fig. 2a).

Effect of C_{60} dosage

Figure 3a shows the cyclic voltammogram results for varying the amount of C_{60}/CH_2Cl_2coated onto a 3 mm GC electrode surface via the SC method. The peak current of the reduction wave was found to increase with an increasing volume of C_{60}/CH_2Cl_2, and exhibits a wider distribution of peak potential and a broader peak. As has been mentioned earlier, reduction of solid C_{60} in 0.1 M K^+ always give rise to a cyclic voltammogram waveform with three peaks. The qualitative pattern and the magnitude of these three peaks depends largely on the C_{60} dosage under similar experimental conditions.

The appearance of a single, but relatively large, reduction wave for C_{60} films in the presence of KCl has been reported previously using a SC technique [16, 17]. However, in this work, three peaks are observed instead. The result of this work (Fig. 3) shows that the C_{60} dosage ranging between 2 μL and 80 μL of 150 μM affects the peak heights but does not affect the number of peaks formed. It appears that a small amount of 2 μL of 150 μM C_{60} is sufficient to produce K_nC_{60} with $n > 1$, as long as a sufficient negative overpotential is applied. However, further experiments using a dosage that is lower than 2 μL of 150 μM C_{60} and a replicating experiment by using another GC electrode were not carried out. However, when a much thicker coating is employed via the MA method (Fig. 1), a different peak formation is observed as compared with that obtained via the SC method. The varying peak formation characteristics can usually be attributed to the varying density of arrays of microcrystalline C_{60}, or varying "thickness" of the C_{60} coating used [14]. Presumably, the different dosage of 2 μL and 80 μL of 150 μM obtained via the SC method is not large enough to affect the number of peaks formed, while the different deposition technique employed will affect it (see above).

At a dosage below 5 μL C_{60}/CH_2Cl_2, two reduction peaks (i) and (ii) appear at −1.4 and −1.5 V, respectively, with extended reductive limiting current of up to −1.8 V. The appearance of peak (i) persisted and peak (ii) increased significantly at the expense of peak (i) with increasing C_{60} dosage of up to 80 μL. Formation of the third reduction peak (iii) begins to be observed at −0.17 V at a C_{60} dosage of greater than 10 μL. Saturation of electrode surface (3 mm diameter GC) with C_{60} is detected at 70 μL upwards as the three reductive peak heights appear nearly constant. This is in good agreement with the results obtained from a similar study carried out in non-aqueous media of acetonitrile (0.1 M NBu_4PF_6). Due to the effect of electrode with limiting surface area, *A* , any increase in the amount of sample that saturates the electrode surface will not further enhance the peak.

Figure 3b shows the total charge transferred, *Q* (calculated from the surface area under CV waveform, from −1300 to –1800 mV), and the number of electrons transferred, *n* , versus the amount of C coated using the SC method. Evidently as more $C_{60}$is coated onto an electrode surface, the density of microcrystal per unit surface area increases. *Q* also increases while the number of electrons transferred (*n*) may decrease from 6 to 1. The use of 20 μL of 150 μM C_{60}/CH_2Cl_2(equivalent to 4.3×10^{-8} mol cm^{-2}, compare with Szs data, $n = 3$ when the density is 8.5×10^{-8} mol cm^{-2}) has a better chance of producing K_3C_{60}. Note that a mixed fulleride may also be formed since the charge transfer process may not be a simple one-electron one-step reduction and that a chemical reaction is coupled to an electrochemical reaction [15].

Effect of the nature of anions and cations in the electrolytes

The type of anion used in an aqueous supporting electrolyte exerts negligible influence on the reduction peak potential of C_{60} (Fig. 4). This observation is similar to those reported in non-aqeous solvent [20] and by other researcher [15, 16, 17, 18, 19]. Figure 4 shows that, in general, redox peaks of C_{60} have a similar pattern of peak formation, with the exception of KNO_3 whose peak (ii) shifts upwards, limited by the working potential range. By investigating the numerical data, the reduction of C_{60} produces only a slight shift of less than 50 mV in K^+-containing electrolyte bearing a different anion. This may be attributed to the varying conductivity and diffusion coefficient (Table 1) [25] rather than the kinetics of the phase transformation. It is because the reduction process of microcrystalline C_{60} only involves the uptake of cation, K^+ and not the anion [7, 8, 9, 10] (see below).

When different Group I alkali-metal cations were used in the solution phase, the electrochemical reduction of C_{60}prepared by the SC method showed a significant variation. The most obvious change occurs in the reduction potential, as shown in Table 2 and Fig. 5. It is clear that when the size of cation decreases, the C_{60} reduction potential shifts to a less negative region. Thus,

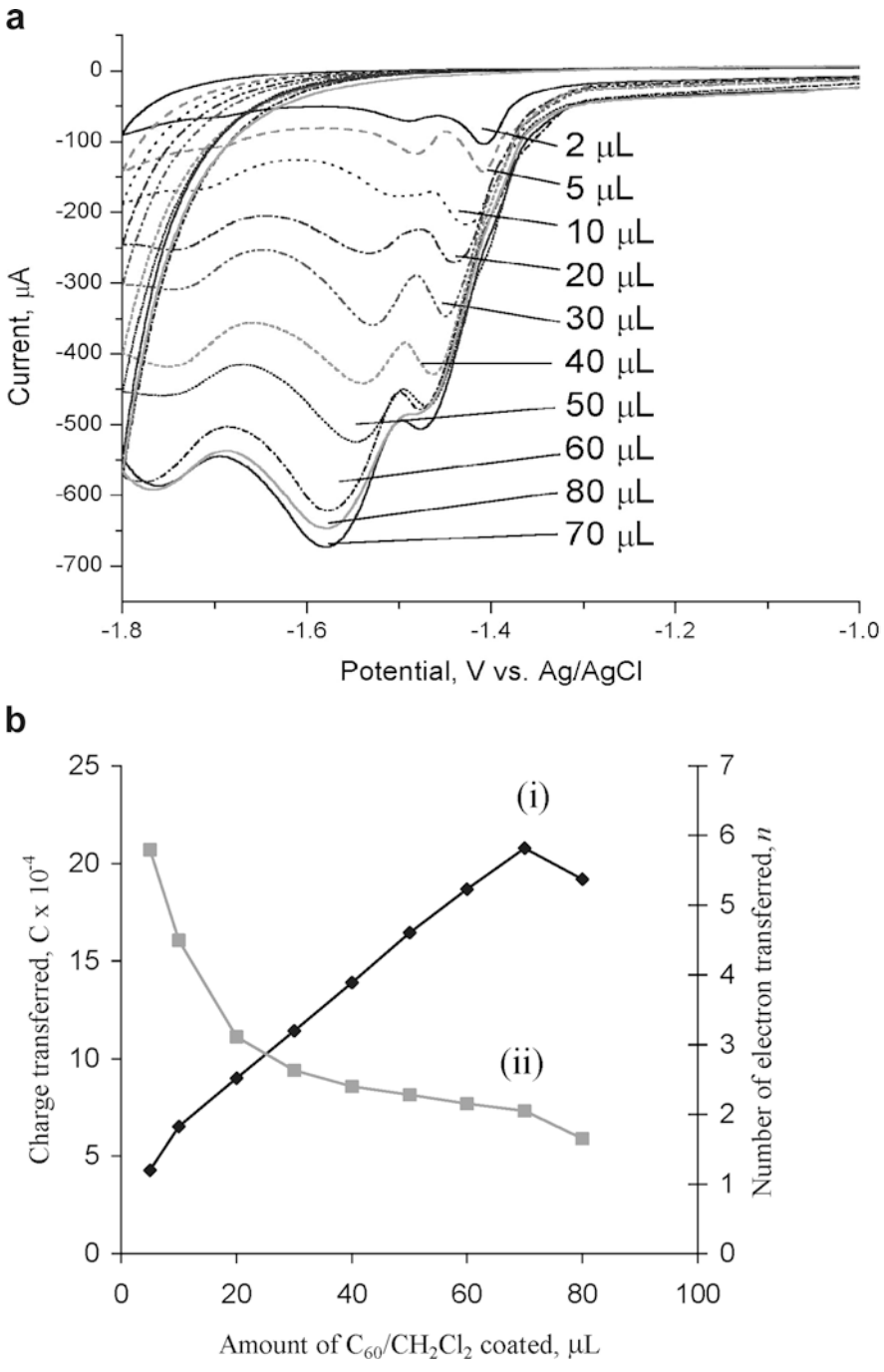

Fig. 3 a Cyclic voltammograms of varying quantity (in volume, μL) of C_{60} solvent cast on a 3 mm diameter GC electrode surface and immersed in 0.1 M KCl; scan rate, 100 mV/s. **b** (i) Total charge transferred and (ii) number of electrons transferred per molecule, n , vs. the varying amount of C_{60}/CH_2Cl_2 coated on a 3 mm diameter GC electrode surface and immersed in 0.1 M KCl; scan rate, 100 mV/s

the size of cation increases and peak reduction potential becomes more negative in the following order: $Li^+ > Na^+ > K^+ > Rb+ > Cs^+$.

To explain this, one must take into consideration the electrochemical factors (such as conductivity and transport number) as well as the thermodynamic variations (such as enthalpy and free energy), which are affected by the sizes of cations. Based on thermodynamics, it is expected that any difference in radius of cation would have influence on the hydration enthalpy, which will produce a change in Gibbs energy and electrical potential as summarized in Tables 2 and 3 [26, 27]. If the hydration energy of a cation is more negative than others, it is then predicted to have a more negative reduction peak potential. The result of this work, as summarized in the above series, shows excellent agreement with theory (Tables 2 and 3). This is different from the results reported earlier by Szücs et al., who found that the peak position of fullerene doped with $Cs^+$was between K^+ and Na^+[16].

Our experimental data showed that a typical cyclic voltammogram of C_{60} attached by the SC method reduced in 0.1 M KCl and RbCl exhibiting three peaks as described earlier (Fig. 1b) but exhibiting only a single peak with a large reduction current for those reduced in 0.1 M CsCl, NaCl, and $LiClO_4$ (Fig. 5).

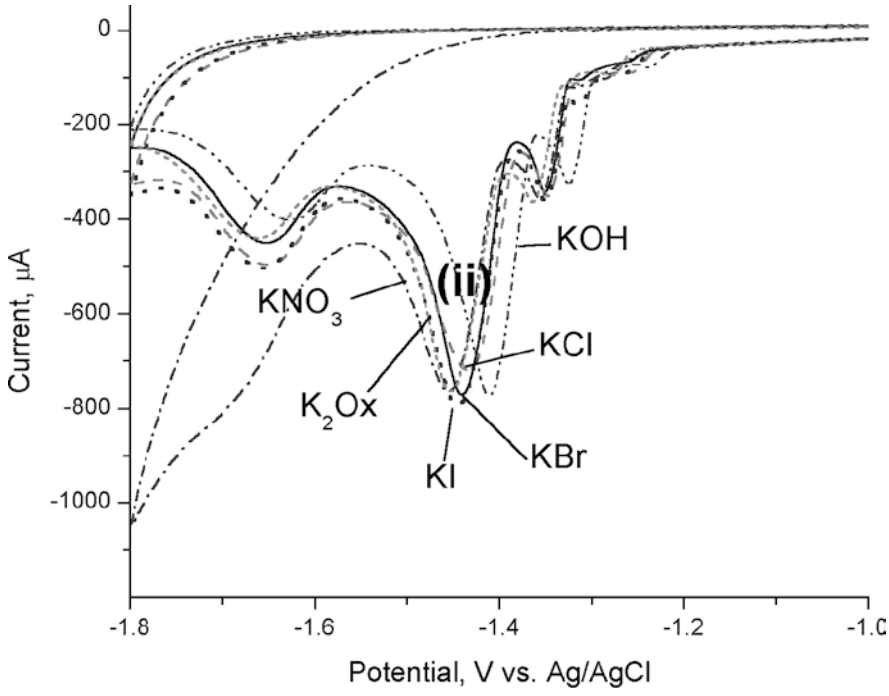

Fig. 4 Effect of varying the anion of the supporting electrolyte on the cyclic voltammograms of 60 μL C_{60}/CH_2CL_2 solvent cast on a 3 mm diameter GC electrode surface. Electrolyte used were 1.0 M KX aqueous solutions were X = Br^-, Cl^-, I^-, NO_3^-, OH^- and 0.5 M K_2Ox; scan rate, 100 mV/s

Under the same conditions, there is no conclusive evidence of a direct relationship between the number of peaks appearing in the cyclic voltammogram and the cation size of supporting electrolyte used. Since the change from single peak to three peaks was not consistent with the increase or decrease in cationic size, the actual reason for the appearance of three peaks and a single peak in this particular case is not clear. Other effects due to the crystal sizes of M_nC_{60} or orientation of related crystal lattices may play a role.

Evidently, those compounds formed lost their faradaic activity soon after the reduction step as no re-oxidation current on the reverse scan and further cycling, even in media containing different types of cations. The Group I alkali-metal fullerides formed, M_nC_{60}(M = Cs^+, Rb^+, K^+, Na^+, and Li^+) are all found to be non-electro-active in water after the electrolysis.

Table 1 Reduction peak potential E_{pc} (ii) of 20 μL C_{60} coated onto GC electrode (3 mm diameter), reduced in 1.0 M KX (X = Cl, Br, I, NO_3, OH) and 0.5 M K_2Ox using scan rate of 100 mV/s

Anion	Limiting ionic conductivities[a] 10^{-4}×Sm^2 mol^{-1}	Ionic diffusion at infinite dilution[a] 10^{-5} cm^2 s^{-1}	E_{pc} for peak (ii) mV
OH^-	198	5.273	−1,410
Cl^-	76.31	2.032	−1,432
Br^-	78.1	2.080	−1,440
I^-	76.8	2.045	−1,445
$(Ox)^{2-}$	-	-	−1,455
NO_3^-	71.42	1.902	−1,458

[a]From [25]

Table 2 Reduction peak potential E_{pc} (ii) of C_{60} (SC) in 0.1 M alkali-metal salts in water, using GC electrode (3 mm diameter) with scan rate of 100 mV/s

Cation	E_{pc} mV
Cs^+	−1,470
Rb^+	−1,500 (ii)
K^+	−1,520 (ii)
Na^+	−1,577
Li^+	−1,865

Effect of varying the amount of supporting electrolyte, KCl

Figure 6 shows the cyclic voltammogram waveforms of C_{60} reduced in KCl of various concentrations ranging from 0.05 to 2.0 M. In higher concentration of KCl (2 M), the three reduction peaks of C_{60} observed earlier are found to have better peak resolution than those obtained in a lower concentration of KCl (0.05 M). The cathodic peak wave of C_{60} shifts in a positive direction as the concentration of the electrolyte increases. This indicates that a smaller reductive overpotential is required for the reduction of C_{60} in the presence of excess electrolyte. The presence of an excess amount of K^+ definitely helps in a more complete reduction of adhered C_{60} microcrystals as the formation of K_nC_{60} becomes kinetically and thermodynamically more favorable. Since ion pairing, asymmetry and electrophoretic effects are easily felt at a higher concentration of electrolyte, a moderate range of 0.1–1.0 M supporting electrolyte is sufficient in most of the voltammetric experiments.

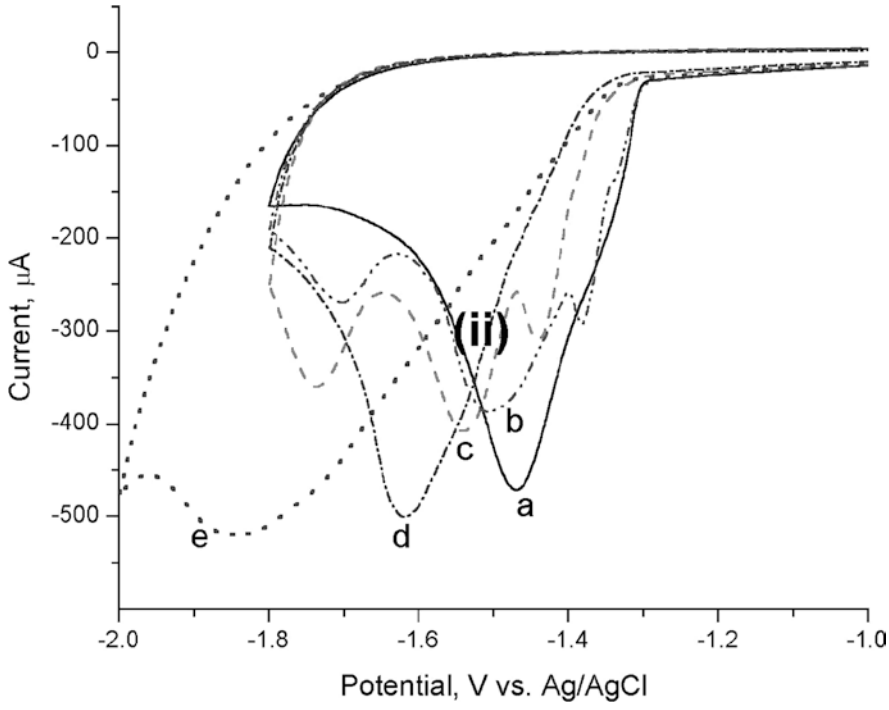

Fig. 5 Effect of varying the alkaline cation of the supporting electrolyte on the cyclic voltammograms of 40 μL C_{60}/CH_2CL_2 solvent cast on the electrode surface of GC and placed in contact with 0.1 M of (a) CsCl, (b) RbCl, (c) KCl, (d) NaCl and (e) $LiClO_4$. Scan rate, 100 mV/s

Table 3 Comparison of crystal, hydrated ion radii, ionic conductivities, and hydration enthalpies for various first class alkali-metal cations [26, 27]

Cation	Crystal radii, r_i Å	Effective hydrated ion radii, r_s Å	Limiting ionic conductivities S cm^2 $equiv^{-1}$	Hydration enthalpies kJ mol^{-1}
Cs^+	1.69	3.29	77.3	−263
Rb^+	1.48	3.29	77.8	−296
K^+	1.33	3.31	73.5	−321
Na^+	0.95	3.58	50.1	−405
Li^+	0.60	3.82	38.7	−515

Effect of mixed supporting electrolyte

In these experiments the electrochemical reduction of C_{60}/CH_2Cl_2coated onto 3 mm GC was studied in solution containing two types of supporting electrolytes, namely CsCl:KCl with different cations of various composition, but the total concentration for the solution remain unchanged. With this technique, it is possible to synthesize mixed alkali-metal fullerides by using various compositions of mixed supporting electrolytes, as reported by Szucs et al.[18].

Figure 7 show the irreversible reduction waveform of C_{60} in 1.0 M KCl without the presence of any other cationic dopant. Again the three reduction peaks were observed. However, when Cs^+ was added to KCl in increasing amount in the order of 2:8, 5:5, and 8:2 (CsCl:KCl), the number of reduction peaks gradually diminished from three to one and the peak potentials for the overall waveforms shifted in a more positive direction. The cyclic voltammogram assumes the character of $Cs_n C_{60}$ fulleride when the Cs dopant is increased (compare Fig. 7b–d with Fig. 7e). Mixed fullerides, $K_xCs_yC_{60}$, probably obtained via ion exchange reactions between the K^+ in the reduced fulleride with the Cs^+ added. A similar trend was reported for the other mixed electrolytes [18, 19].

Effect of scan rate

Figure 8 shows the cyclic voltammogram waveforms of 20 μL C_{60}/CH_2Cl_2at various scan rates reduced in aqueous solution containing 0.1 M KCl using 3 mm GC. The result shows that the current of cathodic wave increases with an increasing scan rate.

Based on the scan rate study of C_{60}in non-aqueous electrolyte, namely NBu_4^+/ACN, it is observed that the rate of current increase is more rapid at slower scan rate than at the faster one; the same behavior is also observed in aqueous electrolyte of K^+. This shows a linear scan rate dependence at a moderate scan rate of 100 mV/s. At higher scan rate, the current increases more slowly, indicating that the surface species are involved in the reactions (surface-confined process), and the wide potential range (the peak broadened) of the electrochemical transformation suggests that they

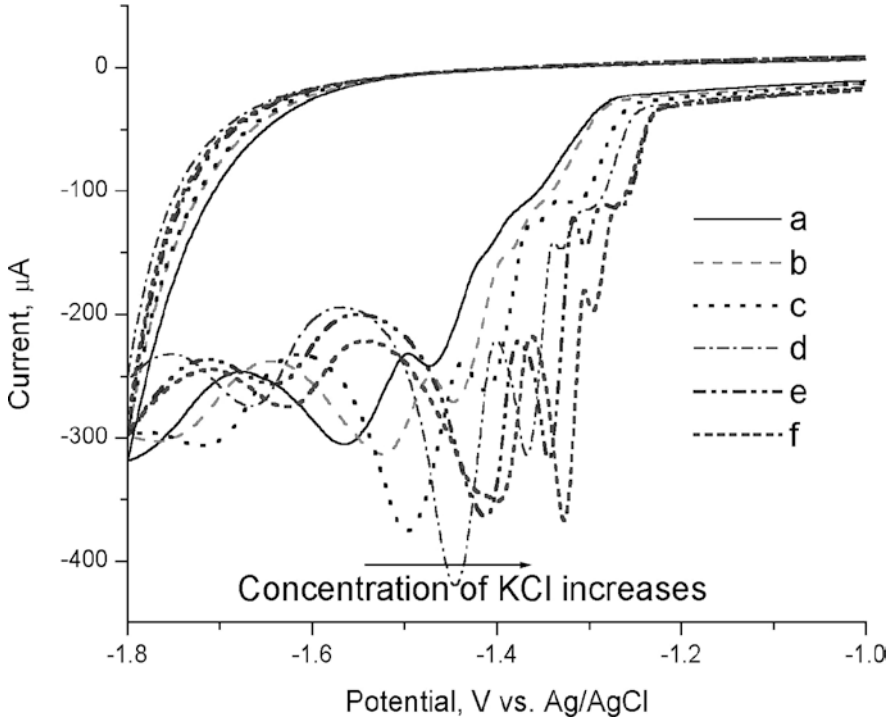

Fig. 6 Effect of varying the concentration of KCl supporting electrolyte on the cyclic voltograms of 20 μL C_{60}/CH_2Cl_2 solvent cast on a 3 mm diameter GC electrode: (a) 0.05 M, (b) 0.1 M, (c) 0.2 M, (d) 0.5 M, (e) 1.0 M, (f) 2.0 M of KCl using a scan rate of 100 mV/s

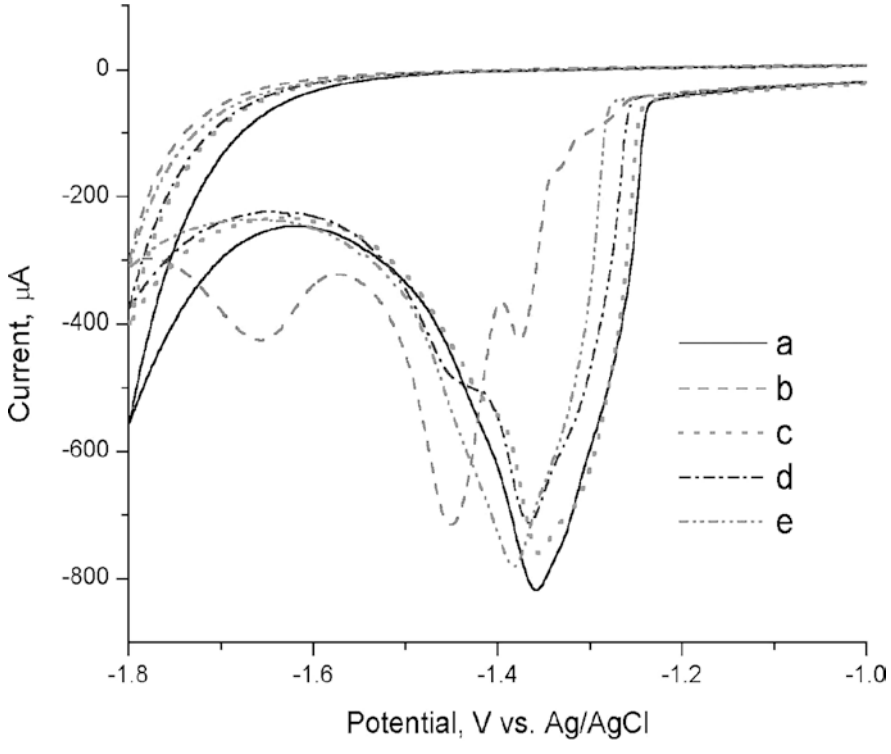

Fig. 7 Cyclic voltammograms of 60 μL C_{60}/CH_2Cl_2 solvent cast on a 3 mm diameter GC electrode surface, and immense in various media of CsCl and KCl: (a) 1.0 M CsCl, (b) 1.0 M KCl, (c) to (e) 1.0 M mixed supporting electrolyte of CsCl: KCl with ratio of (c) 8:2, (d) 5:5, and (e) 2:8

have a broad energy distribution [16]. The plot of peak potential of peak (i) versus scan rate is not linear. It may be due to the formation of mixed fullerides, which contain various values of n (n is the number of electron transfer) rather than a single compound in pure phase [18,19].

Chronocoulometry of C_{60}

A double-step chronocoulometric experiment was carried out for C_{60} attached to a GC electrode via solvent casting, and in contact with 1 M KCl aqueous electrolyte. It consists of an initial potential step from

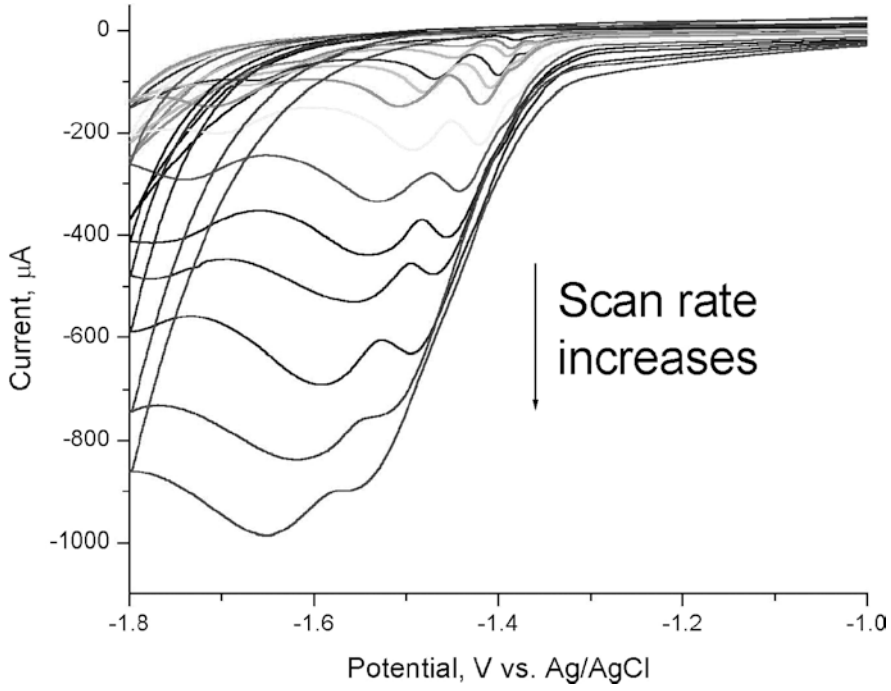

Fig. 8 Effect of varying the scan rate on the cyclic voltammograms of 20 mL C_{60}/CH_2Cl_2 solvent cast on a 3 mm diameter GC electrode surface and immersed in 0.1 M KCl using scan rates of 5, 10, 20, 30, 50, 70, 100, 150, 200, 300, 400, and 500 mV/s

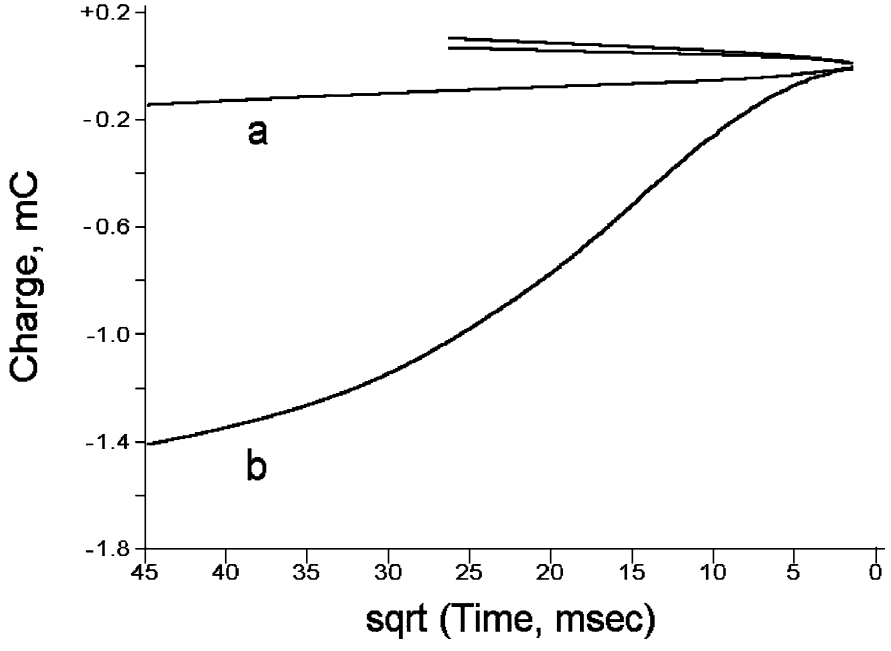

Fig. 9 Charge vs. square root of time of double step chronocoulmmetry for *a* background, *b* 20 μL C_{60}/CH_2Cl_2 coated on a 3 mm diameter GC electrode surface, in 0.1 M KCl using a pulse width of 2,000 msec, potential step from –200 to –1800 mV

−200 to −1800 mV and a reverse step from −1800 mV to −200 mV. Figure 9 is an Anson plot, which shows that during the reduction of C_{60} there is an initial rapid increase in charge with time, corresponding to reduction of most of the surface-confined C_{60} microcrystals. However, during the re-oxidation step there is an absence of electroactivity, as is evident because its charge vs. square root of time line coincides with the background line. The observation confirmed the presence of a surface- based irreversible redox process of C_{60} in the presence of K^+-containing aqueous electrolyte.

Scanning electron microscopic study

Reduction of C_{60} microcrystals in K^+-containing aqueous electrolyte formed typical and shapely microcrystals of K_nC_{60}, fulleride with sizes ranging from 1 to 5 μm (Fig. 10b), slightly larger in size than those

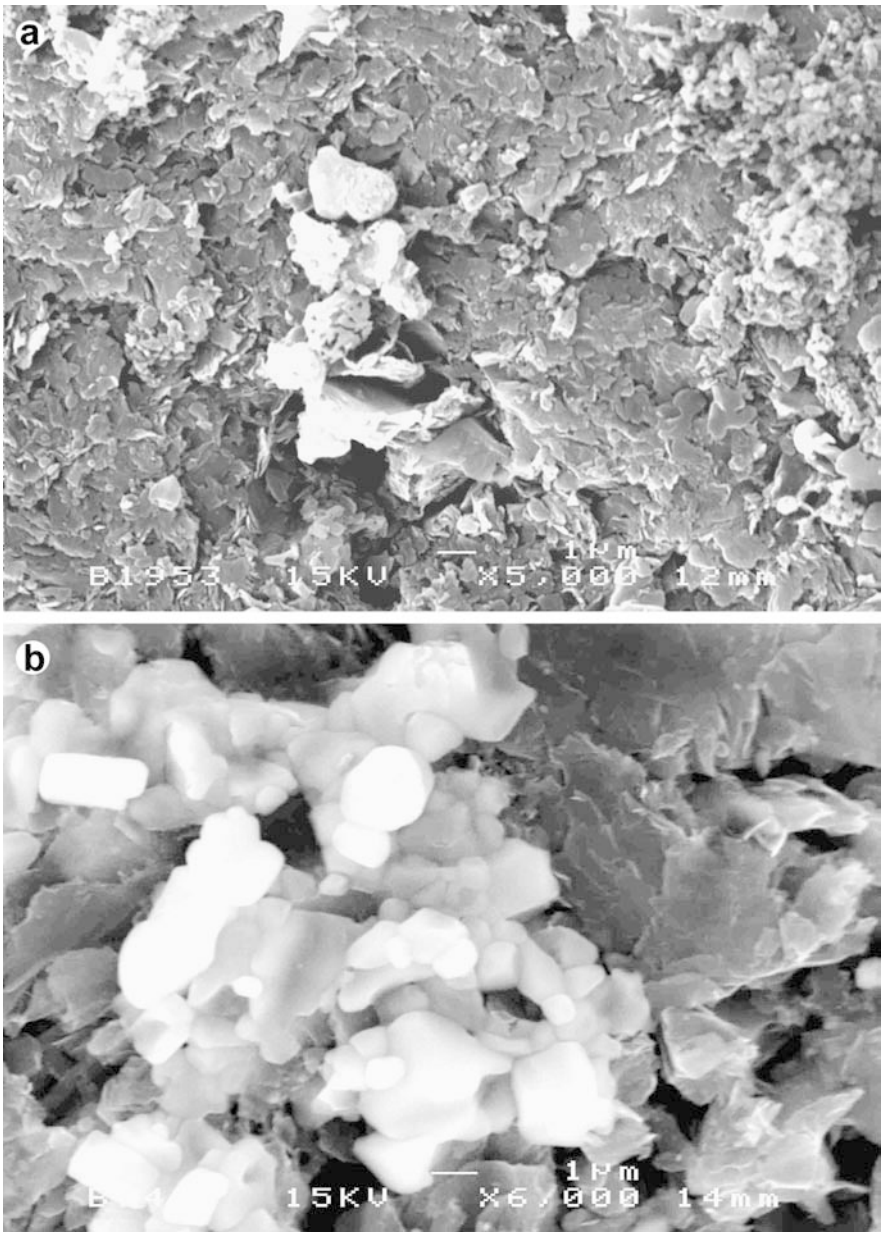

Fig. 10a, b Scanning electron micgrograph of C_{60} microcrystals via solvent cast onto a 5 mm diameter basal plane pyrollitic graphite electrode **a** before electrochemical reduction, **b** after electrochemical reduction at –1800 mV vs Ag/AgCl using 0.1 M KCl aqueous electrolyte

obtained before electrolysis, with size ranging from ca. 3 μm (Fig. 10a) indicating the presence of a surface process of solid–solid transformation.

Conclusions

A reductive potential scanning of an array of microcrystals of C_{60} attached to a GC electrode and immersed in aqueous solution containing potassium ions causes an irreversible electrochemical reduction of C_{60} over the potential range of −1.3 to −1.8 V (vs. Ag/AgCl) with no re-oxidation wave on the reverse scan. Electroactivity of $C_{60}^{0/n-}$ is lost in subsequent potential cycling, indicating a complete reduction of C_{60} solids during the first potential cycle. Evidence is obtained favoring the irreversible intercalation of cationic dopant in the lattices of $C_{60}^{0/-}$ [9,10], forming a passive coating of fullerides rather than the dissolution process [11]. An interesting observation was made that, after the chemically irreversible reduction of C_{60} in water, it remains electrochemically active after transfer to acetonitrile. The pattern of a cyclic voltammetric waveform for C_{60}reduced in K^+ -containing aqueous electrolyte is also affected by the method of transferring C_{60}, namely mechanical attachment (MA) or solvent casting (SC), and the type and concentration of cation, but independent of the type of anion present in the supporting electrolyte, under similar voltammetric conditions. The linear dependence of scan rate on peak height and the chronocoulometric data and the slightly larger crystal size, observed after reduction of C_{60}, indicates the

presence of a surface process involving solid–solid transformation.

Acknowledgement The authors wish to thank Universiti Putra Malaysia and Ministry of Science, Technology and Environment for a research fund sponsored under IRPA research program and a PASCA scholarship for LEB.

References

1. Haufler RE, Conceicao J, Chibante LPF, Chal Y, Byne NE, Flanagan S, Haley MM, O'Brien SC, Pan C, Xiao Z, Billups WE, Ciufolini MA, Hauge RH, Margrave JL, Wilson LJ, Curl RF, Smalley RE (1990) J Phys Chem 94:8634
2. Allemand PM, Koch A, Wudl F, Rubin Y, Diederich F, Alvarez MM, Anz SJ, Whetten RL (1991) J Am Chem Soc 113:1051
3. Cox DM, Behal S, Disko M, Gorun SM, Greaney M, Hsu CS, Kollin EB, MillarJ, Robbins W, Sherwood RD, Tindall P (1991) J Am Chem Soc 113:2940
4. Dubois D, Kadish KM, Flanagan S, Haufler RE, Chibante LPF, Wilson LJ (1991) J Am Chem Soc 113:4364
5. Dubois D, Kadish KM, Flanagan S, Wilson LJ (1991) J Am Chem Soc 113:7773
6. Xie Q, Péréz-Cordero E, Echegoyen L (1992) J Am Chem Soc 114:3978
7. Jehoulet C, Bard AJ, Wudl, F (1991) J Am Chem Soc 113:5456
8. Jehoulet C, Obeng YS, Kim YT, Zhou, F, Bard AJ (1992) J Am Chem Soc 114:4237
9. Compton RG, Spackman RA, Wellington RG, Green MLH, Turner J (1992) J Electroanal Chem 327:337
10. Compton RG, Spackman RA, Riley DJ, Wellington RG, Eklund JC, Fisher AC, Green MLH, Doothwaite RE, Stephens AHH, Turner J (1993) J Electroanal Chem 344:235
11. Tatsuma T, Kikoyama S, Oyama N (1993) J Phys Chem 97:12067
12. Nishizawa M, Tomura K, Matsue T, Uchida I (1994) J Electroanal Chem 379:233
13. Carlisle JJ, Wijayawardhana CA, Evans TA, Melaragno PR, Ailin-Pyzik IB (1996) J Phys Chem 100:15532
14. Suàrez MF, Marken F, Compton RG, Bond AM, Miao W, Raston CL (1999) J Phys Chem B 103:5637
15. Szücs A, Loix A, Nagy JB, Lamberts L (1995) J Electroanal Chem 397:191
16. Szücs A, Loix A, Nagy JB, Lamberts L (1996) J Electroanal Chem 402:137
17. Szücs A, Tesi M, Novák M, Nagy JB, Lamberts L (1996) J Electroanal Chem 419:39
18. Szücs A, Tesi M, Szücs E, Nagy JB, Novák M (1997) J Electroanal Chem 429:27
19. Szücs A, Tesi M, Csiszár M, Nagy JB, Novák M (1998) J Electroanal Chem 442:59
20. Tan WT, Lim EB, Bond AM (2003) J Solid State Electrochem 7:134
21. Balch AL, Costa DA, Fawcett WR, Winkler K (1997) J Electroanal Chem 427:137
22. Bond AM, Miao WJ, Raston CL, Ness TL, Barnes NJ, Atwood AL (2001) J Phys Chem B 105 (9):1687
23. Szucs A, Budavari V, Nagy JB, Novak M (2002) J Electroanal Chem 528:153
24. Oyama M (2002) Electroanalysis 14 (4):277
25. CRC (1997) Handbook of chemistry and physics.
26. Burgess J (1988) Ions in solutions: basic principles of chemical interactions. Ellis Horwood, Chichester
27. Conway BE (1981) Ionic hydration in chemistry and biophysics. Elsevier, Amsterdam